

HIGH RESOLUTION 4.7 μm KECK/NIRSPEC SPECTRA OF PROTOSTARS. II: DETECTION OF THE ^{13}CO ISOTOPE IN ICY GRAIN MANTLES¹

A.C.A. BOOGERT², G.A. BLAKE³, A.G.G.M. TIELENS^{4,5}

To appear in ApJ 577 n1, 20 Sept. 2002 (submitted 6 April 2002; accepted 29 May 2002)

ABSTRACT

The high resolution ($R=25,000$) infrared M band spectrum of the massive protostar NGC 7538 : IRS9 shows a narrow absorption feature at 4.779 μm (2092.3 cm^{-1}) which we attribute to the vibrational stretching mode of the ^{13}CO isotope in pure CO icy grain mantles. This is the first detection of ^{13}CO in icy grain mantles in the interstellar medium. The ^{13}CO band is a factor of 2.3 narrower than the apolar component of the ^{12}CO band. With this in mind, we discuss the mechanisms that broaden solid state absorption bands. It is shown that ellipsoidally shaped pure CO grains fit the bands of both isotopes at the same time. Slightly worse, but still reasonable fits are also obtained by CO embedded in N_2 -rich ices and thermally processed O_2 -rich ices. In addition, we report new insights into the the nature and evolution of interstellar CO ices by comparing the very high resolution multi-component solid ^{12}CO spectrum of NGC 7538 : IRS9 with that of the previously studied low mass source L1489 IRS. The narrow absorption of apolar CO ices is present in both spectra, but much stronger in NGC 7538 : IRS9. It is superposed on a smooth broad absorption feature well fitted by a combination of CO_2 and H_2O -rich laboratory CO ices. The abundances of the latter two ices, scaled to the total H_2O ice column, are the same in both sources. We thus suggest that thermal processing manifests itself as evaporation of apolar ices only, and not the formation of CO_2 or polar ices. Finally, the decomposition of the ^{12}CO band is used to derive the $^{12}\text{CO}/^{13}\text{CO}$ abundance ratio in apolar ices. A ratio of $^{12}\text{CO}/^{13}\text{CO}=71\pm 15$ (3σ) is deduced, in good agreement with gas phase CO studies (~ 77) and the solid $^{12}\text{CO}_2/^{13}\text{CO}_2$ ratio of 80 ± 11 found in the same line of sight. The implications for the chemical path along which CO_2 is formed are discussed.

Subject headings: Infrared: ISM—ISM: molecules—ISM: abundances—stars: formation—stars: individual (NGC 7538 : IRS9)—astrochemistry

1. INTRODUCTION

Ever since the detection of interstellar solid CO (Soifer et al. 1979; Lacy et al. 1984) in the 4.67 μm spectra of protostars and background objects, the absorption band profile has been used as a diagnostic of the composition and evolution of interstellar ices (Whittet, McFadzean, & Longmore 1985; Sandford et al. 1988; Tielens et al. 1991; Chiar et al. 1998; Teixeira, Emerson, & Palumbo 1998). The absorption band was found to consist of a narrow feature accompanied by a broader feature at longer wavelengths. With the help of laboratory simulations it was found that the broad component is due to CO mixed with H_2O ('polar' ices) and the narrow feature due to pure CO or CO mixed with apolar species such as O_2 , N_2 or CO_2 . The relative depth of the apolar and polar ices is thought to reflect thermal processing in the envelopes of protostars, because these ices have quite different sublimation temperatures (18 K versus 90 K respectively). Also, the knowledge gained from observing the interstellar CO band is invaluable in studying the outgassing behavior of cometary ices as comets approach the sun (Sandford &

Allamandola 1988).

We have therefore started a program to measure the interstellar CO ice band at very high spectral resolution ($R=25,000$), more than an order of magnitude higher than customary until now, using the NIRSPEC spectrometer at the Keck II telescope. In Paper I of this program, we presented the spectrum of the low mass protostar L1489 IRS in the Taurus molecular cloud (Boogert, Hogerheijde, & Blake 2002). At the high spectral resolution we discovered a new, third, CO component on the short wavelength side of the absorption band, which is compatible with absorption by CO_2 -rich CO ices. Combining the ice observations with information obtained from the gas phase CO lines in the same spectrum, we concluded that the CO ices are thermally processed in the upper layers of the circumstellar disk surrounding L1489 IRS. In this Paper, we present the high resolution M band spectrum of the massive protostar NGC 7538 : IRS9. This source has a rich and well studied infrared ice band absorption spectrum (Whittet et al. 1996). The ices are thought to reside in a thick and young circumstellar envelope, surrounding a modest hot core where the ices have evaporated (Mitchell et al. 1990). Indeed, large gas phase depletion factors

¹ The data presented herein were obtained at the W.M. Keck Observatory, which is operated as a scientific partnership among the California Institute of Technology, the University of California and the National Aeronautics and Space Administration. The Observatory was made possible by the generous financial support of the W.M. Keck Foundation.

² California Institute of Technology, Department of Astronomy 105-24, Pasadena, CA 91125, USA; acab@astro.caltech.edu

³ California Institute of Technology, Division of Geological and Planetary Sciences 150-21, Pasadena, CA 91125, USA

⁴ Kapteyn Astronomical Institute, P.O. Box 800, 9700 AV Groningen, the Netherlands

⁵ SRON, P.O. Box 800, 9700 AV Groningen, the Netherlands

are needed in envelope models explaining millimeter wave emission lines toward NGC 7538 : IRS9 (van der Tak et al. 2000). The contribution of ice absorption from unrelated cold foreground clouds in the NGC 7538 complex is likely small given the weakness of ice bands toward nearby protostars with more evolved envelopes (e.g. NGC 7538 : IRS1; Lacy et al. 1984). The CO ice band toward NGC 7538 : IRS9 has a large apolar component, tracing unprocessed ices in the cold envelope (Sandford et al. 1988; Tielens et al. 1991; Chiar et al. 1998), and thus forms an interesting contrast with L1489 IRS. In addition to the ^{12}CO band we report the first detection of solid ^{13}CO in NGC 7538 : IRS9 (and in the interstellar medium in general), providing an independent tracer of the composition of apolar ices. It also offers a reliable way of measuring the interstellar carbon isotope ratio, in follow up to measurements of the solid $^{12}\text{CO}_2/^{13}\text{CO}_2$ ratio obtained with the *Infrared Space Observatory* (ISO; Boogert et al. 2000), and to gas phase measurements (see Wilson & Rood 1994).

This Paper is structured as follows. The observations and data reduction procedure are described in §2. The 2092 cm^{-1} absorption band is identified with solid ^{13}CO in §3.1.1 using laboratory spectra. In §3.1.2 we compare the apolar component of the ^{12}CO band with the ^{13}CO band, explaining the factor 2.3 wider ^{12}CO band. After isolating the apolar component of the ^{12}CO band from the underlying broader absorption, we derive the interstellar solid $^{12}\text{CO}/^{13}\text{CO}$ abundance ratio in §3.2. The astrophysical implications of these results are discussed in §4. A refined picture for the processing of CO ices is presented in §4.1. By comparing solid $^{12}\text{CO}/^{13}\text{CO}$ and $^{12}\text{CO}_2/^{13}\text{CO}_2$ isotope ratios we discuss the chemical pathway leading to the formation of interstellar CO_2 in §4.2.

2. OBSERVATIONS

The massive protostar NGC 7538 : IRS9 was observed with the NIRSPEC spectrometer (McLean et al. 1998) at the Keck II telescope atop Mauna Kea on UT 2001 August 8. During the observations the sky was clear and dry, and the seeing was good ($\sim 0.5''$ at 2.2 μm). NIRSPEC was used in the echelle mode with the $0.43 \times 24''$ slit, providing a resolving power of $R = \lambda/\Delta\lambda = 25,000$ ($\sim 12 \text{ km s}^{-1}$) with three Nyquist sampled settings covering the wavelength ranges 4.624–4.699 μm , 4.684–4.756 μm , and 4.754–4.822 μm in the atmospheric M transmission band.

The data were reduced in a standard way, using IDL routines. The thermal background emission was removed by differencing the nodding pair. Each nodding position was integrated on for 2 minutes, before pointing the telescope to the other nodding position. A correction for residual sky emission was performed by subtracting neighboring rows from the stellar spectrum. The most critical step in the reduction of this data is the correction for atmospheric absorption features. For this purpose the standard star HR 8585 (A1V) was observed, which is bright ($V=3.78$) and reasonably close to NGC 7538 : IRS9 (an airmass of 1.20 versus 1.34 for NGC 7538 : IRS9). The spectral shape and hydrogen absorption features in the standard were divided out with a Kurucz model atmosphere. After ratioing the standard and NGC 7538 : IRS9 spectra, an overall good telluric correction was achieved, resulting in final signal-to-noise values of respectively ~ 40 , 60, and 70

on the unsmoothed data, for integration times of 6, 12, and 26 minutes on each of the three settings. The noise determination takes into account small imperfections in the cancellation of the multitude of weak telluric features, which we believe are the limiting factor in the achievable signal-to-noise for this bright object ($M \sim 3$ magn.; Whittet et al. 1996). Regions with strong atmospheric lines, i.e. with less than 50% of the maximum transmission in each setting, leave residuals and were removed from the final spectrum. This does not affect the interstellar CO lines because at the time of the observations these lines are shifted by as much as -82 km s^{-1} with respect to the deep telluric CO lines. The spectra were wavelength calibrated on the atmospheric CO emission lines, and subsequently the three settings were combined by applying relative multiplication factors. We have not attempted to flux calibrate the spectrum, since we are interested in absorption features only.

The longest wavelength setting was also observed on two other nights (UT 2001 August 7 and UT 2002 January 3). The presence, depth and profile of the weak absorption feature of ^{13}CO , the topic of this paper (§3), are confirmed in these independent data. We do not present these data here, because of their overall reduced quality due to shorter integration time (2001 August) and poor system performance (2002 January).

3. RESULTS

The most prominent feature in the $R=25,000$ spectrum of NGC 7538 : IRS9 is absorption by solid ^{12}CO in the frequency range 2125–2150 cm^{-1} (Fig. 1). A much weaker and narrower absorption feature is present at 2092 cm^{-1} , which is ascribed to the stretching mode of solid ^{13}CO (see §3.1.1). Throughout the full 2074–2164 cm^{-1} frequency range absorption lines originating from the ro-vibrational transitions of ^{12}CO , ^{13}CO , and C^{18}O are present. The ^{12}CO lines also show an emission component on the red shifted side, increasing in strength for higher rotational J levels. Some of the higher J level ^{13}CO lines have emission components as well. The gas phase features have previously been analyzed in Mitchell et al. (1990). Our study will therefore focus on the analysis of the ice features.

We study the ice features on an optical depth scale. The continuum on the long wavelength side of the ^{12}CO ice feature is smoothly rising and can be fitted with a straight line. The apparent continuum slope on the short wavelength side is, however, significantly steeper. Most likely this is because of the presence of an additional ice absorption band due to the stretching mode of a triply bonded CN-bearing species, the so-called ‘XCN’ band. Indeed, low resolution spectral studies report the presence of this band toward NGC 7538 : IRS9 centered at 4.62 μm (Lacy et al. 1984; Chiar et al. 1998; Pendleton et al. 1999). We therefore chose to extrapolate the straight line continuum defined at high wavelength toward lower wavelengths. This results in an ‘XCN’ absorption feature with an optical depth of $\tau=0.13$ at 4.62 μm . This is less than the value of 0.31 quoted in Pendleton et al. (1999), which we believe is mainly ($\Delta\tau=0.1$) due to contamination by blended, unresolved gas phase CO lines in their low resolution spectrum, but also partly due to the lack of short wavelength continuum in our spectrum.

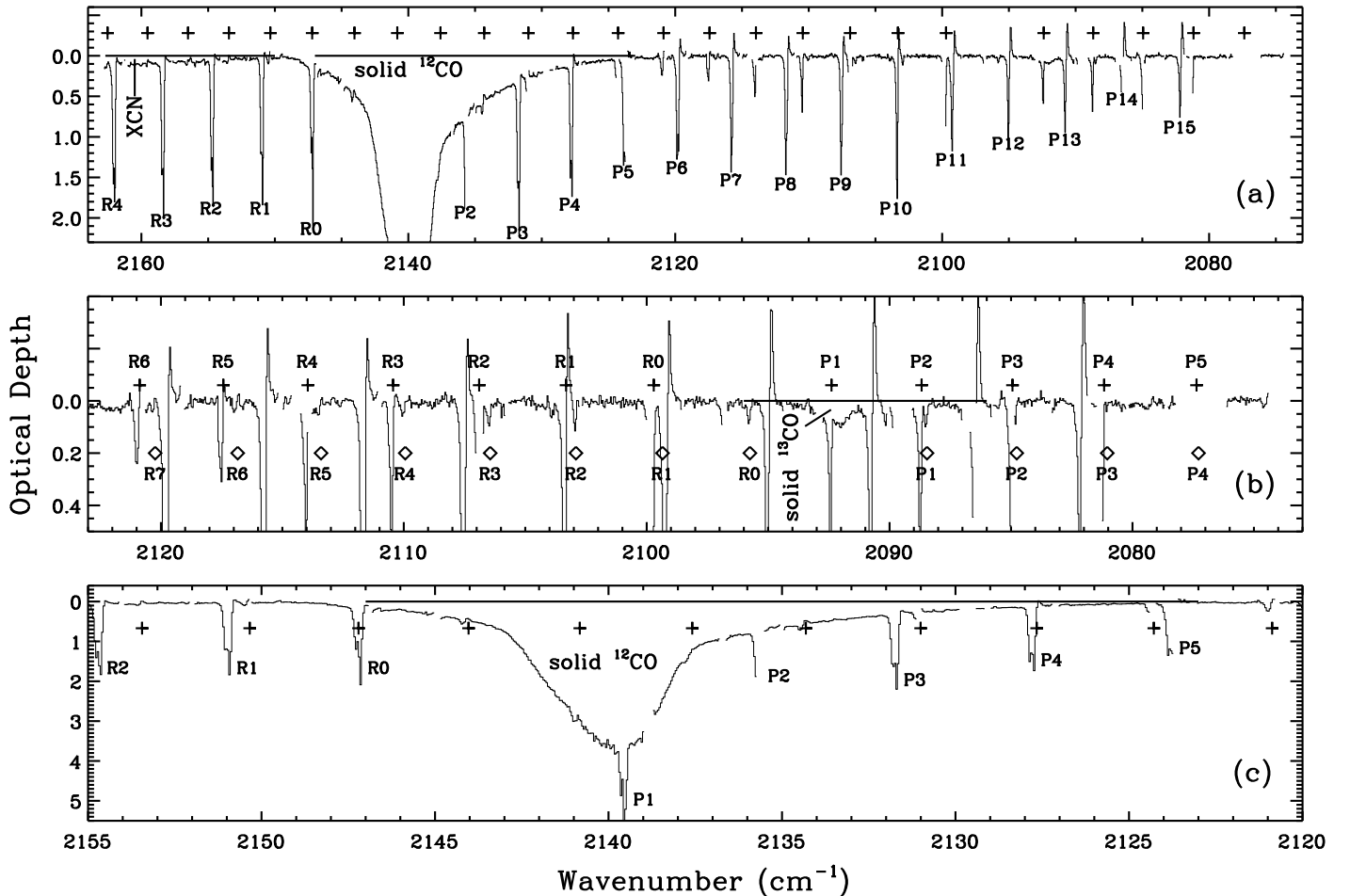


FIG. 1.— Observed, unsmoothed, $R=25,000$ M band spectrum of NGC 7538 : IRS9 on an optical depth scale, with identifications of gas phase ^{12}CO (deepest narrow lines), gas phase ^{13}CO ('+' symbols above spectrum), part of the shallow 'XCN' band, and solid ^{12}CO (panel a). A portion of the spectrum is enlarged in panel b, showing in detail the absorption band of solid ^{13}CO at 2092 cm^{-1} along with the absorption lines of gas phase ^{13}CO ('+' symbols) and C^{18}O (diamonds). The emission component on the red shifted side of the deep high J level ^{12}CO absorption lines are real. Panel c shows in detail the deep absorption band of solid ^{12}CO . The presence of the P(1) line in the trough of the ice absorption band indicates that the ice band is not saturated. All plotted spectra are corrected for object and earth velocity (-82 km s^{-1}). Wavelength regions with poor atmospheric transmission are not plotted, causing the gaps in the spectra.

Although little flux is left in the bottom of the solid ^{12}CO band, this band is not saturated as is shown by the presence of the P(1) line of gaseous ^{12}CO in the bottom of the ice band (Fig.1). The peak optical depth of the solid ^{12}CO band is $\tau(\text{CO})=3.6\pm 0.2$, an important number for our isotope ratio determination (§3.2). The uncertainty of 0.2 is determined from three difference nodding pairs, and shows the data is reliable even in extremely deep absorption bands. However, $\tau(\text{CO})$ is significantly larger than the value of 2.6 previously reported (Lacy et al. 1984; Tielens et al. 1991). This is partly explained by instrumental broadening of the narrow apolar CO band by the previous low resolution spectrometers. We calculate that the depth of the CO band would be reduced by $\Delta\tau(\text{CO})=0.6$ and 0.3 at the resolution of the data in Lacy et al. (1984) and Tielens et al. (1991) respectively. An additional uncertainty may result from the continuum determination in the presence of many unresolved strong gas phase CO absorption lines.

The newly detected absorption band of solid ^{13}CO is an independent tracer of the composition of icy grain mantles. Its identification is discussed in §3.1.1. Extra information

is obtained by comparing the ^{13}CO band with the apolar component of the ^{12}CO band (§3.1.2). In §3.2 we derive the $^{12}\text{CO}/^{13}\text{CO}$ isotope ratio in interstellar ices, for which a new approach to decompose the polar and apolar ^{12}CO ice components is introduced. The astrophysical implications of these results are discussed in §4.

3.1. New Constraints on the Composition of Apolar Ices

3.1.1. Identification of Interstellar Solid ^{13}CO

In order to characterize the absorption feature detected at 2092 cm^{-1} in the spectrum of NGC 7538 : IRS9, Gaussian fits were carried out. We find a peak frequency of $\nu=2092.30\pm 0.21\text{ cm}^{-1}$, a peak optical depth of $\tau=0.089\pm 0.010$, and a width of $\text{FWHM} = 1.50\pm 0.45\text{ cm}^{-1}$ (3σ errors). At the NIRSPEC resolving power of $R = 25,000$ ($\Delta\nu = 0.084\text{ cm}^{-1}$) the feature is well resolved, and fortunately well separated from the forest of surrounding interstellar and telluric gas phase absorption and emission features. Features providing the greatest interference are the unresolved P(1) absorption line of interstellar gaseous ^{13}CO at 2092.39 cm^{-1} and a telluric feature at slightly larger frequency. The deepest part of the tel-

luric feature was removed from the data. Despite these limitations, the fitted Gaussian parameters are similar in the observations made on the three different nights (§2).

The laboratory experiments on solid CO from the works of Ehrenfreund et al. (1997) were used with the goal of identifying the 2092 cm^{-1} feature with absorption by solid ^{13}CO and to further constrain the composition of interstellar ices. These laboratory spectra have the high spectral resolution (1.0 cm^{-1}) and signal-to-noise required to study the band profile of the weak and narrow ^{13}CO feature. Other relevant laboratory studies, such as the $\text{N}_2:\text{CO}$ experiments of Elsila, Allamandola, & Sandford (1997) and the pure CO study of Baratta & Palumbo (1998) unfortunately lack sufficient spectral resolution to resolve and characterize the ^{13}CO feature.

The laboratory profiles of the ^{13}CO stretching mode were analyzed in a way similar to that done for ^{12}CO (Boogert et al. 2002). After a careful baseline subtraction, the peak position and width were determined as a function of ice composition and temperature. Generally, the same trends found for the ^{12}CO band are recognized in ^{13}CO (Fig. 2). The band of ^{13}CO in a pure amorphous CO ice peaks at 2092.3 cm^{-1} and is very narrow ($\text{FWHM}=1.5\text{ cm}^{-1}$). An extreme broadening and shift to larger wavelengths are observed when CO is mixed with H_2O ice, because of the large dipole moment of the H_2O molecules. Similarly large effects are expected for other astrophysically relevant molecules with large dipole moments (CH_3OH , NH_3), but no laboratory experiments are available for these mixtures at present. Mixtures of CO with the apolar species CO_2 , and to a lesser degree with O_2 , can also give drastically broadened ^{13}CO bands. A fragile amorphous structure is formed between the CO molecules and CO_2 and O_2 , providing an absorption feature that is broadest at mixing ratios of 1:1 (Ehrenfreund et al. 1997). Upon warming this structure is destroyed and the band narrows, although in particular for CO_2 mixtures the width is still larger than that of a pure CO ice. In contrast, only a very small broadening is observed in mixtures of CO with N_2 , even at 1:1 mixing ratios ($\text{FWHM}=1.8\text{ cm}^{-1}$). Finally, the peak position does not shift in mixtures of CO with O_2 , but the ^{13}CO band (as well as the ^{12}CO band) shifts by $0.5\text{--}1\text{ cm}^{-1}$ to shorter wavelengths when mixed with CO_2 and by 0.5 cm^{-1} when mixed with N_2 .

Using these results, we conclude that the peak and width of the 2092 cm^{-1} absorption feature observed toward NGC 7538 : IRS9 are best explained by the stretching mode of ^{13}CO in a pure CO ice (Fig. 3b and d). At low laboratory temperatures, only small amounts (less than 10% in total) of H_2O , CO_2 , and/or O_2 are allowed in the ices. Larger concentrations would violate the observed narrow width. A laboratory CO spectrum with 16% CO_2 content at a laboratory temperature of $T=10\text{ K}$ can already be excluded, for example (Fig. 4b). At higher laboratory temperatures, CO_2 mixtures still poorly match the observations. In O_2 mixtures, the band narrows sufficiently at higher temperatures ($\sim 30\text{ K}$) to give reasonable fits even at large O_2 concentrations ($> 50\%$; Fig. 4d and f). Finally, the mixture $\text{N}_2:\text{CO}=1:1$ gives a somewhat poorer fit to the observed ^{13}CO band because of a $\sim 0.5\text{ cm}^{-1}$ shift to shorter wavelengths (Fig. 4h). However, we consider

this mixture still reasonable because of the good fit to the ^{12}CO band (§3.1.2).

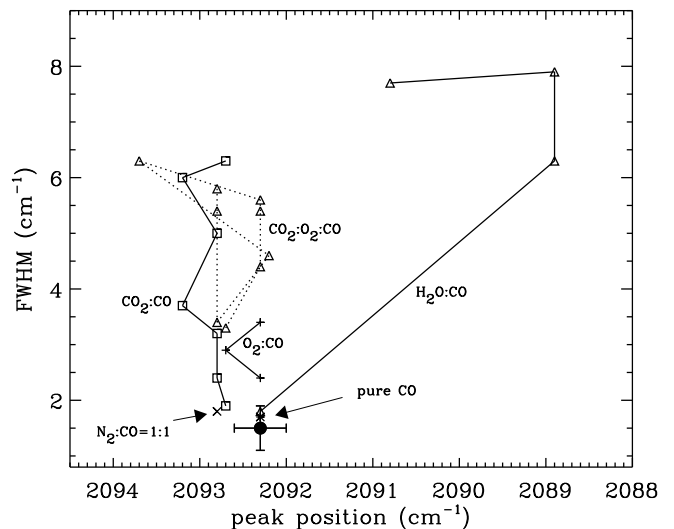


FIG. 2.— Diagram showing the effect of ice composition on the peak position and width of the solid ^{13}CO stretching mode, as determined from laboratory experiments. The CO concentration decreases upwards along each curve. In mixtures with CO_2 and/or O_2 a maximum width is achieved at CO concentrations of 50%. The width dependence is much smaller for N_2 mixtures. The dot with the error bars represents the observed peak position and width of the absorption feature detected toward NGC 7538 : IRS9, which is best fit by a pure CO ice, or by CO-rich ices with trace amounts ($\sim 10\%$) of CO_2 , O_2 , and/or H_2O .

3.1.2. Comparison of ^{12}CO and ^{13}CO Band Profiles

The profile of the solid ^{12}CO band toward NGC 7538 : IRS9 is dominated by a prominent narrow absorption centered at 2140 cm^{-1} . It shows also absorption on an extended long wavelength wing, as well as in a wing to the short wavelength side (Fig. 1). Broad wing absorption is not detected in the present signal-to-noise limited spectrum of the ^{13}CO band of NGC 7538 : IRS9. The origin of the ^{12}CO wings and the decomposition from the central narrow component is further discussed in §3.2. Here we will concentrate on a comparison of the ^{13}CO absorption with the narrow 2140 cm^{-1} ^{12}CO component, which must, given their small width, both originate from apolar ices. The width of the ^{12}CO feature ($\text{FWHM}=3.5\text{ cm}^{-1}$) is a factor of 2.3 ± 0.7 (3σ) larger than the width of the ^{13}CO band. What mechanism(s) can make the interstellar ^{12}CO band broader than the ^{13}CO band?

The width of absorption bands of molecules embedded in solid matrices is affected by a number of difficult to disentangle mechanisms. In experiments of CO isolated in annealed N_2 matrices, the width of the CO bands was found to depend strongly on the CO/N_2 ratio (Dubost, Charneau, & Harig 1982). This ‘concentration broadening’ is the result of shifts in the transition frequency because of static and dynamic interactions between the CO molecules themselves. The static interaction is due to the electric field generated by the permanent dipole moment of one CO molecule working on other nearby CO molecules or due to the electric field created by crystalline defects. The dynamic interaction is due to the resonance of oscillating electric fields generated by different CO molecules.

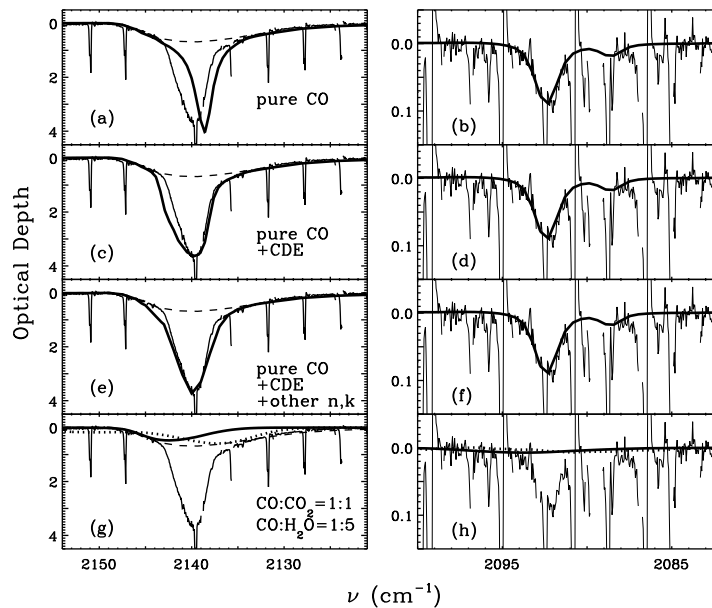


FIG. 3.— Observed ^{12}CO (left panels) and ^{13}CO (right panels) absorption bands of NGC 7538 : IRS9, fitted by laboratory and calculated spectra of solid CO (thick lines; normalized to observed peak optical depth). For the ^{12}CO band the shallow over-plotted spectrum (dashed line) represents a fit to the long and short wavelength wings of NGC 7538 : IRS9 obtained from the observed spectrum of L1489 IRS (see Fig. 5d). Panels **a** and **b** show added to this the pure CO ice spectrum observed in transmission in the laboratory (Ehrenfreund et al. 1997), which clearly does not fit the ^{12}CO band. Panels **c** and **d** also show a pure CO ice, but now assuming absorption by ellipsoidal grains (‘CDE’ model) providing a much better fit. Panels **e** and **f** show the same grain model, using the optical constants of Baratta & Palumbo (1998) for ^{12}CO (but ^{13}CO from Ehrenfreund et al. 1997). Panels **g** and **h** show a fit to the short and long wavelength wings of ^{12}CO by $\text{CO}:\text{CO}_2=1:1$ (thick solid line) and $\text{CO}:\text{H}_2\text{O}=1:5$ (dots) mixtures respectively, which have a negligible contribution to the ^{13}CO absorption band.

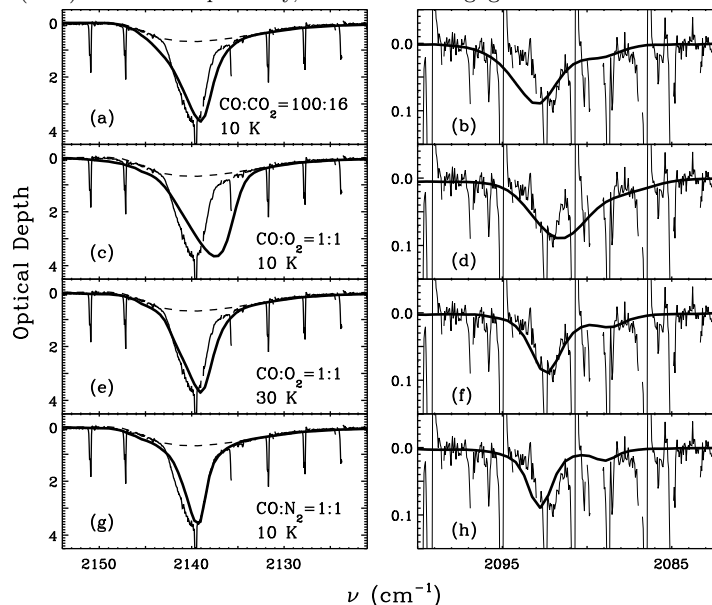


FIG. 4.— Same as for Fig. 3, but now for comparing the apolar component in NGC 7538 : IRS9 with various laboratory mixtures. Panels **a** and **b** show the mixture $\text{CO}:\text{CO}_2=100:16$ as observed in transmission in the laboratory. Panels **c** and **d** show the mixture $\text{CO}:\text{O}_2=1:1$ at $T=10\text{ K}$, while panels **e** and **f** show the same mixture at $T=30\text{ K}$. Panels **g** and **h** show $\text{CO}:\text{N}_2=1:1$. The effect of particle shape corrections is small for all mixtures, except for the ^{12}CO band in $\text{CO}:\text{CO}_2=100:16$. We conclude that all these mixtures give poorer fits to the observations compared to pure CO spectra (Fig. 3), but $\text{CO}:\text{O}_2=1:1$ (provided it is thermally processed) and $\text{CO}:\text{N}_2=1:1$ are still considered reasonable.

The frequency shifts induced in both cases result in broadening of the absorption band because of the distribution of the local field generated by the different configurations of the neighboring molecules. The smallness of the permanent dipole moment of CO makes the broadening from dynamic interaction significantly larger than broadening induced by static interaction. This greatly enhances the width of the ^{12}CO band with respect to the ^{13}CO band,

because the concentration of ^{12}CO molecules is a factor of 90 higher. There is no dynamic interaction of ^{13}CO with ^{12}CO molecules, because their transition frequencies are several tens of wavenumbers apart. Thus, at a mixing ratio of $\text{CO}:\text{N}_2=1:100$, the band of ^{12}CO was found to be a factor of 5 wider than the ^{13}CO band (Dubost et al. 1982). However, at such a low CO concentration the bands of both isotopes are an order of magnitude too nar-

row compared to the bands observed toward NGC 7538 : IRS9. At higher CO concentrations, the width of both bands increases, but that of the ^{12}CO band grows more slowly because the dynamic and static broadening mechanisms are not additive, and in fact the static fields detune the dynamic interactions. As a result, a pure, annealed CO ice has an FWHM=1.7 cm^{-1} for ^{12}CO , and FWHM=1.1 cm^{-1} for ^{13}CO (Ewing & Pimentel 1961; Dubost et al. 1982). These widths increase by $\sim 0.5 \text{ cm}^{-1}$ when the CO ice structure is amorphous (Sandford et al. 1988). Thus, a pure CO ice that may be amorphous provides a good fit to the ^{13}CO band (FWHM=1.5 cm^{-1}) observed toward NGC 7538 : IRS9, but this pure CO ice has a ^{12}CO band that is still a factor of 1.60 too narrow.

An additional mechanism is therefore needed that can selectively broaden the ^{12}CO band. A viable mechanism is interaction of light with CO-rich interstellar icy grains. Electromagnetic radiation can polarize the ^{12}CO dipoles, which induces electric fields within the grain that oscillate at the ^{12}CO vibration transition frequency (e.g. Bohren & Huffman 1983). This creates resonances with the dipole electric field, resulting in frequency shifts and band broadening, but only at sufficiently high CO concentrations (>30%; Tielens et al. 1991). Therefore, the profile and position of the band of the diluted ^{13}CO molecules are not affected by these particle shape effects. Using the calculations in the small particle limit presented in Ehrenfreund et al. (1997), we thus find that acceptable fits to the ^{12}CO band are obtained for ellipsoidally shaped particles, in particular with a continuous distribution of shapes ('CDE'; Fig. 3c). Although there is a mismatch on the short wavelength side of the 2140 cm^{-1} feature, this can be accounted for by assuming other particle shapes or by uncertainties in the optical constants of CO. A better fit is obtained (Fig. 3e) if we take the slightly different optical constants of Baratta & Palumbo (1998). Note that the shape of the ^{13}CO band indeed remains unchanged for different particle shapes (Fig. 3b and d).

Finally, an alternative way to preferentially broaden the ^{12}CO band is to change the ice composition. In the database of Ehrenfreund et al. (1997) the ratio of ^{12}CO to ^{13}CO band width is ~ 1.3 for most mixtures. At low laboratory temperatures ($T = 10 \text{ K}$) the mixture $\text{N}_2:\text{CO}=1:1$ has the largest width ratio (1.5), while at high laboratory temperatures ($T = 30 \text{ K}$) mixtures with $\text{O}_2/\text{CO} \geq 1$ have width ratios of up to 1.8. The N_2 mixture provides the best fit to the ^{12}CO band, and the heated O_2 mixture fits the ^{13}CO band better (§3.1.1; Fig. 4e–h). We thus consider these mixtures as reasonable, but not as good as pure CO.

To conclude, the peak position and width of the ^{13}CO band observed in the direction of NGC 7538 : IRS9 are well explained by a pure CO ice that might be amorphous. To fit the ^{12}CO band with the same pure ice a mechanism is needed that preferentially broadens the ^{12}CO band. Interaction of light with small particles has this effect. It also shifts the ^{12}CO band to the observed peak position. Alternatively, the observed band widths and peak positions are reasonably matched with $\text{N}_2:\text{CO}=1:1$ ices or thermally processed O_2 -rich ices. Whether the *required* mild degree of thermal processing of O_2 ices is realistic in the NGC 7538 : IRS9 line of sight is further discussed in §4.1.

3.2. Deriving the $^{12}\text{CO}/^{13}\text{CO}$ Isotope Ratio in Interstellar Ices

In order to determine an accurate $^{12}\text{CO}/^{13}\text{CO}$ ratio it is necessary to correct the ^{12}CO absorption band for absorption in its extended wings. This requires knowledge of the intrinsic shape of the absorption features responsible for the apparent wings. Insight is gained by comparing the observed ^{12}CO profile of NGC 7538 : IRS9 with that of the low mass protostar L1489 IRS (Boogert et al. 2002). The two spectra have similarly high signal-to-noise values at the same high spectral resolution, allowing a detailed comparison. The absorption in the wings is much more prominent in L1489 IRS with respect to that of the central 2140 cm^{-1} peak (Fig. 5a). It is found that the ^{12}CO profile of NGC 7538 : IRS9 can be excellently reproduced by multiplying the L1489 IRS spectrum with a factor of 1.5 to match the wings (Fig. 5b), and adding a Gaussian with peak $\nu = 2139.8 \text{ cm}^{-1}$, width FWHM=3.5 cm^{-1} (§3.1.2) and an optical depth of 2.4 (Fig. 5c). This implies that the central 2140 cm^{-1} absorption and the wings are spectroscopically independent CO ice components. We can now determine the intrinsic shape of the absorption in the wings by *subtracting* the same Gaussian—but different optical depth—from the observed L1489 IRS profile. The main uncertainty here is the depth of the Gaussian. Two extreme cases can be distinguished: a relatively small correction of $\tau = 0.4$ (corresponding to 0.6 when scaled to the wings of NGC 7538 : IRS9) such that a smooth profile remains, or a factor of two larger correction such that the optical depth at 2140 cm^{-1} is zero and two separate long

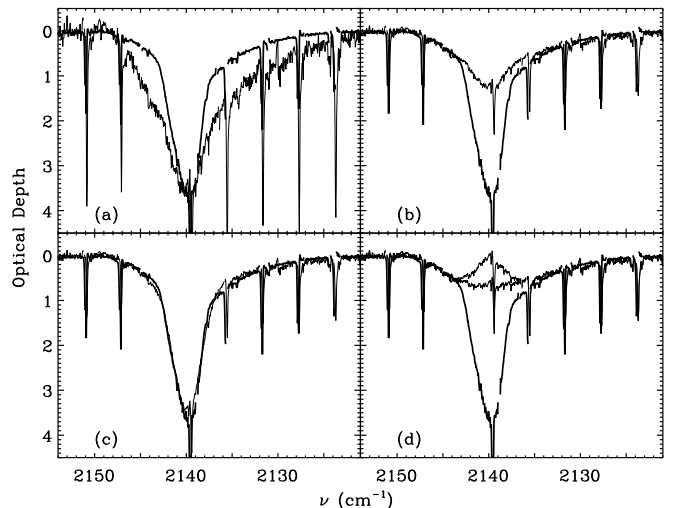


FIG. 5.— Comparison of the ^{12}CO spectrum of NGC 7538 : IRS9 (thick line in each panel) to that of the low mass protostar L1489 IRS (thin lines; Boogert et al. 2002), providing insight into the nature of this band. In panel **a** the L1489 IRS spectrum is scaled to the peak optical depth of the NGC 7538 : IRS9 spectrum by multiplication with a factor of 4.3. In panel **b** the wings of L1489 IRS are scaled to the wings of NGC 7538 : IRS9, by multiplication with a factor of 1.5. In panel **c** the NGC 7538 : IRS9 spectrum is excellently reproduced by adding to the scaled L1489 IRS spectrum a Gaussian with a peak optical depth of $\tau=2.4$. In panel **d** the central narrow peak in L1489 IRS is corrected for in two different ways by subtracting the same Gaussian with $\tau=0.6$ and $\tau=1.2$ respectively from L1489 IRS (see text for more details). In each panel, the narrow absorption lines superposed on the ice spectra are due to gas phase CO in the same line of sight.

and short wavelength absorption features remain (Fig. 5d). We argue that the former case is most likely, because with the presently available database of laboratory spectra it is impossible to obtain two separate absorption features. As discussed in Boogert et al. (2002), the long wavelength wing of the ^{12}CO band is very likely due to CO diluted in H_2O -rich ices (see also Tielens et al. 1991; Chiar et al. 1998), while the short wavelength wing is well fitted with a $\text{CO}:\text{CO}_2$ mixture. Together, they form the smooth broad absorption feature underlying the narrow 2140 cm^{-1} band (however, see §4.1 for an alternative interpretation). Using these laboratory mixtures, and assuming a nominal isotope ratio (see below), it can be seen that the ^{13}CO band in these ices is much broader than the observed 2092 cm^{-1} feature and that the peak optical depth is negligible (Fig. 3g and h).

For the column density and isotope ratio determinations that follow we will therefore assume that the narrow 2140 cm^{-1} component is superposed on a smooth underlying broad absorption feature, the shape of which we determine from the L1489 IRS spectrum as described above. We thus find that the integrated area of the narrow 2140 cm^{-1} feature toward NGC 7538 : IRS9 is 10.4 cm^{-1} , which is about half the total integrated area (20.2 cm^{-1}). If the second correction method were applicable, the integrated area for the 2140 cm^{-1} feature would be 11% larger.

The column density of ices is derived by dividing the integrated optical depth over the laboratory measured intrinsic band strength A . The band strength⁶ of ^{12}CO was measured to be $A^{12} = 1.1 \times 10^{-17}\text{ cm molecule}^{-1}$ (Jiang, Person, & Brown 1975). The absolute value of A^{13} has not been measured, but its value relative to A^{12} can be determined by measuring the integrated optical depths of the ^{13}CO and ^{12}CO stretching modes in laboratory experiments. Using the pure CO spectrum of Ehrenfreund et al. (1997), and taking into account a laboratory isotope ratio of 89, we thus find that A^{12} and A^{13} are identical. This contradicts the study of Gerakines et al. (1995) which reports that A^{13} is 18% larger than A^{12} . It is likely that Gerakines et al. (1995) included a close-by satellite band at 2088.6 cm^{-1} (Fig. 3) in the integrated optical depth of ^{13}CO (P. Gerakines, private communication). This satellite band, however, must originate from solid C^{18}O , given its position and strength (Ewing & Pimentel 1961). Finally, we find that A^{12} , but not A^{13} , increases with 10% when the spectrum is corrected for absorption by small particles (as was also found by Tielens et al. 1991). In interstellar space this is a realistic case (§4.1), and we therefore conclude that the interstellar isotopic $^{12}\text{CO}/^{13}\text{CO}$ column density ratio is given by

$$\frac{^{12}\text{CO}}{^{13}\text{CO}} = \frac{\tau_{\text{int}}^{12} \times A^{13}}{\tau_{\text{int}}^{13} \times A^{12} \times 1.10} = \frac{\tau_{\text{int}}^{12}}{\tau_{\text{int}}^{13} \times 1.10}, \quad (1)$$

where τ_{int}^{12} and τ_{int}^{13} are the integrated optical depths of the observed ^{12}CO and ^{13}CO bands. Deriving τ_{int}^{13} from the Gaussian fit in §3.1.1, and τ_{int}^{12} with the method described above, we find

$$\frac{^{12}\text{CO}}{^{13}\text{CO}} = 71 \pm 15(3\sigma). \quad (2)$$

The 3σ uncertainty reflects the uncertainty in the peak depth of the ^{12}CO (because of the low signal in the bot-

tom of the feature; §3) and ^{13}CO features. The 30% error in the observed FWHM of ^{13}CO can be neglected if one assumes that a pure CO ice is responsible for the ^{13}CO absorption (FWHM= 1.50 cm^{-1}). A broadening by small amounts of CO_2 , H_2O or O_2 is allowed by the uncertainty in the width of the feature (§3.1.1). This would reduce the isotope ratio by 30% (3σ), i.e. such broadening imposes a lower limit of $^{12}\text{CO}/^{13}\text{CO} > 50$. Another systematic error is the extraction of the 2140 cm^{-1} component from the observed ^{12}CO profile, which could increase the ratio by at most 11%.

4. ASTROPHYSICAL IMPLICATIONS, SUMMARY AND FUTURE WORK

4.1. The Nature and Evolution of CO ices

It has been claimed that CO ices evolve by the heating effects of nearby protostars (Tielens et al. 1991; Chiar et al. 1998). Sources in different evolutionary stages may thus have ices of different composition or structure in their neighborhood. It is also expected that gradients in the physical conditions result in different ices as a function of distance to the protostar. In particular, the abundance ratio of volatile apolar CO ices versus less volatile polar CO ices may reflect the thermal distribution of the dust along the line of sight, much like the structure of polar CO_2 -containing ices traces the thermal evolution of massive protostellar envelopes (Gerakines et al. 1999; Boogert et al. 2000). This might be accompanied by energetic processing of CO ices, resulting in the formation of new species, such as CO_2 and perhaps ‘XCN’ close to the star, although this is less well established.

With the high spectral resolution and high signal-to-noise observations of solid ^{12}CO and ^{13}CO presented in this paper, a refined picture of the evolution of interstellar CO ices can be constructed. The ^{12}CO spectra of NGC 7538 : IRS9 and L1489 IRS (§3.2) can be taken as templates for unprocessed and processed ices respectively (group I and II spectra in the nomenclature of Chiar et al. 1998). In §3.2 it was shown that the unprocessed spectrum of NGC 7538 : IRS9 can be reproduced by simply adding a narrow Gaussian (representing apolar ices at 2140 cm^{-1}) to the processed spectrum of L1489 IRS. Thus, processing manifests itself largely as evaporation of the most volatile ices: the abundance of apolar ices normalized to the H_2O ice column is a factor of 5 lower in the warm upper layers of the L1489 IRS circumstellar disk compared to the cold envelope of NGC 7538 : IRS9 (Table 1). In contrast, the composition, structure, and abundances of the ices responsible for the short and long wavelength wings remain unchanged. Both sources have abundances of 3.5% and 7.5% for the CO ices responsible for these wings respectively. If we assume that the wing at short wavelengths is caused by CO_2 -rich CO ices⁷ (Boogert et al. 2002; consistent with the high CO_2/CO column density ratio; Table 1), then the similar abundance for both sources indicates that CO ice processing does not produce significant quantities of CO_2 molecules. This is sustained by the fact that the position and width of the apolar 2140 cm^{-1} feature is the same

⁶ we will adopt the notation A^{12} and A^{13} for the band strengths of the stretching modes of ^{12}CO and ^{13}CO respectively

⁷ At present there are no laboratory experiments supporting the idea that the same carrier is responsible for both wings.

TABLE 1
COLUMN DENSITIES OF ICES

Species	$N/N(\text{H}_2\text{O}) \times 100\%$		Reference
	NGC 7538 : IRS9	L1489 IRS	
H ₂ O	100	100	1, 2
CO ₂	25	17	3, 4
CO apolar	15	3	5, 6
CO long λ wing	8	7	5, 6
CO short λ wing	4	3	5, 6

References: (1) $N(\text{H}_2\text{O})=64 \times 10^{17} \text{ cm}^{-2}$ from Allamandola et al. 1992; (2) $N(\text{H}_2\text{O})=47 \times 10^{17} \text{ cm}^{-2}$ from Sato et al. 1990; (3) Gerakines et al. 1999; (4) not observed, but assuming the typical value from Gerakines et al. 1999; (5) this work; (6) Boogert et al. 2002

for both objects. The weakness of energetic processing in the presence of strong thermal processing in the L1489 IRS line of sight is also evident by the absence of a strong 2165 cm^{-1} ($4.62 \mu\text{m}$) XCN band (we estimate $\tau[\text{XCN}] \leq 0.14$ taking alternative continua compared to Boogert et al. 2002). The non-correlation of energetically processed ices and (un)processed apolar ices along one line of sight seems to be a common characteristic of interstellar ices (Pendleton et al. 1999; Whittet et al. 2001) and may well reflect a spatial segregation associated with protostellar activity. Finally, the comparison between these different lines of sight does not favor the model in which CO molecules migrate into an underlying porous H₂O ice layer at increased temperatures, because this would result in higher abundances of CO ices responsible for the long wavelength, polar wing (Thi 2002). Of course, these hypotheses must be tested against future high resolution observations of a larger sample of protostars.

Additional constraints on the nature of the apolar CO component are obtained by comparing the ¹²CO and ¹³CO band widths and peak positions. The ¹³CO band is best explained by a pure, perhaps amorphous, CO ice. The apolar component of the ¹²CO band is a factor of 2.3 broader. This may well be caused by interaction of light with randomly oriented CO-rich particles that have a distribution of ellipsoidally shapes (CDE), which broadens the ¹²CO band but leaves the ¹³CO band unchanged. Interestingly, ellipsoidally shaped grains were also found to give best fits to the interstellar CO₂ bands (Gerakines et al. 1999). The CDE distribution mimics irregularly shaped ice grains (Tielens et al. 1991) or grain clustering (Rouleau & Martin 1991).

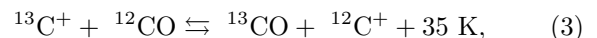
The case that pure CO ices are responsible for the apolar component would imply that at the time of the ice mantle formation the abundance of CO is larger than that of the apolar species O₂ and N₂. It has been argued that pure interstellar CO ices may not be realistic given the large cosmic abundances of O and N (Elsila et al. 1997). The amount of O and N locked up in O₂ and N₂ is, however, poorly constrained. Direct detection of these species in the solid state by their vibrational bands is complicated, and only high upper limits have been derived (Vandenbussche et al. 1999; Sandford et al. 2001). Neverthe-

less, N₂ and thermally processed O₂-rich CO ices give only slightly poorer fits to the ¹³CO and ¹²CO apolar component (§3.1.2; see also discussions in Chiar et al. (1998) and Vandenbussche et al. (1999) for ¹²CO). The laboratory temperature required for the O₂-rich ices to fit the width of the bands of both isotopes is 30 K, close to the sublimation temperature (Fig. 4c-f). At the low vapor pressures and large time scales in interstellar space these temperatures scale down to ~ 18 K (Nakagawa 1980). While it is likely that these conditions occur somewhere in the envelope or NGC 7538 : IRS9, one may question how at these temperatures so close to the sublimation temperature the abundance of apolar ices can be so large. Concluding, although pure CO ices are spectroscopically slightly preferred, from an astrophysical point of view both pure CO, and N₂ containing CO ices, and, less likely, processed O₂-rich CO ices could be the constituents of apolar ices.

4.2. Tracing Chemical Pathways through Isotope Ratios

In this work, we found that the solid ¹²CO/¹³CO abundance ratio is 71 ± 15 (3σ) in the NGC 7538 : IRS9 line of sight (§3.2). This value is in good agreement with the gas phase CO isotope ratio of 78 that is expected at the galactocentric radius of NGC 7538 : IRS9 (9.4 kpc; Wilson & Rood 1994). Furthermore, the isotope ratios for gas and solid CO are similar to that found for solid state ¹²CO₂/¹³CO₂ along the same line of sight (80 ± 11^8 ; Boogert et al. 2000). These values are expected to trace the ‘true’ carbon isotope ratio at this galactocentric radius (see below), which provides constraints on models for the chemical evolution of the Galaxy (Tosi 1982). Also, the isotope ratios provide an independent test for the chemical origin of interstellar CO₂.

Chemical fractionation, or isotope selective destruction, expressed in the isotopic exchange reaction



can greatly change the atomic ¹²C(+)/¹³C(+) ratio even deep within dense clouds. Species derived from atomic C(+) will reflect the enhanced isotope ratio. On the other hand, the isotope ratio of CO, and its chemical daughter products, is not significantly affected by these processes in dense clouds, where CO is the main carbon reservoir.

⁸ The error quoted for the ¹²CO₂/¹³CO₂ ratio represents a systematic error, the 3σ statistical error is less than this.

Within this framework, the carbon isotope ratio of a variety of molecules in dense clouds has been investigated in chemical models (Langer & Graedel 1989). These models show isotope ratios of 120–220 for H_2CO , CS, and HCN compared to 73 for CO. The wide range of values reflects the range of temperatures and densities used in the models. The ratios increase with temperature and density. In the case of NGC 7538 : IRS9, the large abundance of apolar CO ices indicates dust temperatures less than the sublimation temperature (< 18 K; Nakagawa 1980). This would give carbon isotope ratios of trace species of 120–150 at a density of $5 \times 10^3 \text{ cm}^{-3}$. Such densities are realistic in the cold outer parts of the envelope around NGC 7538 : IRS9 (van der Tak et al. 2000). We conclude that while the observed solid $^{12}\text{CO}/^{13}\text{CO}$ ratio is comparable to that of the models, gas phase models in which CO_2 is formed from atomic $\text{C}^{(+)}$ would predict a significantly higher ratio for CO_2 . The similarity of the isotope ratios for solid CO and CO_2 thus indicates, not unexpectedly, that interstellar CO_2 has been formed from CO. This is consistent with proposed grain surface chemistry schemes based upon oxidation of accreted CO (Tielens & Hagen 1982). The absence of CO_2 in the main, 2140 cm^{-1} , apolar CO component of NGC 7538 : IRS9 (§3.1.1) indicates that CO_2 was formed at a different time or location than the apolar CO ice mantles. Indeed, CO_2 was found to be intimately mixed with H_2O (Gerakines et al. 1999), itself a grain surface product. The similarity of the solid CO and CO_2 isotope ratios is also consistent with energetic processing (UV irradiation, cosmic ray hits) of existing CO ice man-

gles (d’Hendecourt et al. 1986), but this is *not* favored by the narrow width of the 2140 cm^{-1} apolar CO component.

While there is little doubt that CO_2 originates from CO, the above discussion illustrates that isotope ratios may provide a powerful way to discriminate between gas phase and grain surface routes for molecules of which the origin is more disputed. In particular, CH_3OH and H_2CO are often assumed to reflect evaporation of ices, even in dark clouds (e.g. Ceccarelli et al. 2001). Their formation on the grain surface probably involved hydrogenation of CO (e.g. Charnley, Tielens, & Millar 1992). Their isotope ratio should thus reflect that of CO. In contrast, gas phase models for the formation of these species rely on C^+ or C broken out of CO through, for example, cosmic ray produced photons. Their isotope ratio is then expected to be quite different (Langer & Graedel 1989). Future accurate determinations of carbon ratios of gas phase H_2CO and CH_3OH and more complex species will therefore be useful in unraveling the interstellar chemical network.

The research of A.C.A.B. and G.A.B. is supported by the SIRTf Legacy Science program and by the Owens Valley Radio Observatory through NSF grant AST-9981546. We thank the anonymous referee for several useful comments. The authors wish to extend special thanks to those of Hawaiian ancestry on whose sacred mountain we are privileged to be guests. Without their generous hospitality, none of the observations presented herein would have been possible.

REFERENCES

- Allamandola, L.J., Sandford, S.A., Tielens, A.G.G.M., & Herbst, T.M. 1992, *ApJ*, 399, 134
 Baratta, G.A., & Palumbo, M.E. 1998, *J.Opt.Soc.Am. A*, 15, 3076
 Bohren, C.F., & Huffman, D.R. 1983, *Absorption and Scattering of Light by Small Particles*. John Wiley & Sons, New York
 Boogert, A.C.A., Ehrenfreund P., Gerakines, P.A., Tielens, A.G.G.M., Whittet, D.C.B., et al. 2000, *A&A*, 353, 349
 Boogert, A.C.A., Hogerheijde, M.R., & Blake, G.A. 2002, *ApJ*, 568, 761
 Ceccarelli, C., Loinard, L., Castets, A., Tielens, A.G.G.M., Caux, E., Lefloch, B., & Vastel, C. 2001, *A&A*, 372, 998
 Charnley, S.B., Tielens, A.G.G.M., & Millar, T.J. 1992, *ApJ*, 399, L71
 Chiar, J.E., Gerakines, P.A., Whittet, D.C.B., Pendleton, Y.J., Tielens, A.G.G.M., Adamson, A.J., & Boogert, A.C.A. 1998, *ApJ*, 498, 716
 d’Hendecourt, L.B., Allamandola, L.J., Grim, R.J.A., & Greenberg, J.M. 1986, *A&A*, 158, 119
 Dubost, H., Charneau, R., & Harig, M. 1982, *Chem. Phys.*, 69, 389
 Ehrenfreund, P., Boogert, A.C.A., Gerakines, P.A., Tielens, A.G.G.M., & van Dishoeck, E.F. 1997, *A&A*, 328, 649
 Elsila, J., Allamandola, L.J., & Sandford, S.A. 1997, *ApJ*, 479, 818
 Ewing, G.E., & Pimentel, G.C. 1961, *J. Chem. Phys.*, 35, 925
 Gerakines, P.A., Whittet, D.C.B., Ehrenfreund, P., Boogert, A.C.A., Tielens, A.G.G.M., et al. 1999, *ApJ*, 522, 357
 Gerakines, P.A., Schutte, W.A., Greenberg, J.M., & van Dishoeck, E.F. 1995, *A&A*, 296, 810
 Jiang, G.J., Person, W.B., & Brown, K.G. 1975, *J.Chem.Phys.*, 62, 1201
 Lacy, J.H., Baas, F., Allamandola, L.J., van de Bult, C.E.P., Persson, S.E., et al. 1984, *ApJ*, 276, 533
 Langer, W.D., & Graedel, T.E. 1989, *ApJS*, 69, 241
 McLean, I.S., Becklin, E.E., Bendiksen, O., Brims, G., & Canfield, J. 1998, *Proc. SPIE*, 3354, 566
 Mitchell, G.F., Maillard, J.-P., Allen, M., Beer, R., & Belcourt, K. 1990, *ApJ*, 363, 554
 Nakagawa, N. 1980, *IAU Symp. 87: Interstellar Molecules*, 87, 365
 Pendleton, Y.J., Tielens, A.G.G.M., Tokunaga, A.T., & Bernstein, M.P. 1999, *ApJ*, 513, 294
 Rouleau, F., & Martin, P.G. 1991, *ApJ*, 377, 526
 Sandford, S.A., & Allamandola, L.J. 1988, *Icarus*, 76, 201
 Sandford, S.A., Allamandola, L.J., Tielens, A.G.G.M., & Valero, G.J. 1988, *ApJ*, 329, 498
 Sandford, S.A., Bernstein, M.P., Allamandola, L.J., Goorvitch, D., & Teixeira, T.C. 2001, *ApJ*, 548, 836
 Sato, S., Nagata, T., Tanaka, M., & Yamamoto, T. 1990, *ApJ*, 359, 192
 Soifer, B.T., Puetter, R.C., Russell, R.W., Willner, S.P., Harvey, P.M., & Gillett, F.C. 1979, *ApJ*, 232, L53
 Teixeira, T.C., Emerson, J.P., & Palumbo, M.E. 1998, *A&A*, 330, 711
 Thi, W.-F. 2000, Ph.D. Thesis. Rijksuniversiteit Leiden
 Tielens, A.G.G.M., & Hagen, W. 1982, *A&A*, 114, 245
 Tielens, A.G.G.M., Tokunaga, A.T., Geballe, T.R., & Baas, F. 1991, *ApJ*, 381, 181
 Tosi, M. 1982, *ApJ*, 254, 699
 Vandenbussche, B., Ehrenfreund, P., Boogert, A.C.A., van Dishoeck, E.F., Schutte, W.A., et al. 1999, *A&A*, 346, L57
 van der Tak, F.F.S., van Dishoeck, E.F., Evans, N.J., & Blake, G.A. 2000, *ApJ*, 537, 283
 Whittet, D.C.B., McFadzean, A.D., & Longmore, A.J. 1985, *MNRAS*, 216, 45P
 Whittet, D.C.B., Schutte, W.A., Tielens, A.G.G.M., Boogert, A.C.A., de Graauw, T., et al. 1996, *A&A*, 315, 357
 Whittet, D.C.B., Pendleton, Y.J., Gibb, E.L., Boogert, A.C.A., Chiar, J.E., & Nummelin, A. 2001, *A&A*, 550, 793
 Wilson, T.L., & Rood, R.T. 1994, *ARA&A*, 32, 191